JOURNAL OF THE BALKAN GEOPHYSICAL SOCIETY, Vol. 2, No 3, August 1999, p. 63-74, 7 figs.

Properties of the magnetotelluric frequency-normalised impedance over a layered medium

Ahmet T. Basokur

Ankara Universitesi, Fen Fakultesi, Jeofizik Muh. B., Tandogan, 06100 Ankara, Turkey.
E-mail: basokur@science.ankara.edu.tr

(Received 21 January 1999; accepted 9 April 1999)

Abstract: *The frequency-normalised impedance (FNI) function is introduced to give a physical significance to the magnetotelluric data. The FNI function is separated into its real and imaginary parts that have the same denominator to estimate their values in the high- and low-frequency limits. The behaviour of the apparent resistivity definitions and the phase is explained theoretically by considering the real and the imaginary parts of the FNI function. The oscillations on the apparent resistivity curves are explained by using ascending and descending types two-layer curves of the FNI function.*

The concept of the reciprocal geoelectric section is developed by using the properties of the FNI function. It has been shown that the apparent resistivity curves of a geoelectric section and those of corresponding to the reciprocal geoelectric section are symmetric. The axis of symmetry is the horizontal axis that intersects the vertical axis at unity.

The FNI function assists the interpreter by giving a clear idea about the number of layers, the resistivity ratio between consecutive layers and it serves a good approximation of the true resistivity values of the subsurface layers.

Key Words: *Frequency-normalized Impedance, Magnetotellurics, Apparent Resistivity Definitions*.

INTRODUCTION

The magnetotelluric (MT) sounding is carried out by measuring the horizontal electric field and the orthogonal horizontal magnetic field versus time. However, the Fourier transformations of the measured field quantities are estimated and the MT data are interpreted in the frequency domain. A ratio of the electric field to the magnetic field yields the impedance in a specified frequency range. The impedance is not directly proportional to the true resistivity distribution of the subsurface. The impedance can be normalised versus frequency to obtain a better representation of the MT response (Basokur, 1994a). This data normalisation versus frequency connects the field ratio to the subsurface structural pattern. In this paper, the merits of the suggested type of data presentation and the use the FNI function for the interpretation of the MT data will be discussed. For simplicity, the discussion will be limited to 1-D situation to examine the behaviour of the FNI function, but similar analysis can be extended to any type of earth structure.

THEORY

The impedance in MT method is given as:

$$Z = E / H \qquad (1)$$

where E and H denote the electric and the orthogonal magnetic fields, respectively. The impedance can be normalised versus frequency as follows:

$$Y = Z / \sqrt{i\omega\mu} = \frac{1}{\sqrt{i\omega\mu}} = \frac{E_x}{H_y} \qquad (2)$$

where ω is the angular frequency, μ is the magnetic

permeability of free space, and *Y* is known as the frequency-normalised impedance function (Basokur 1994a). The notation for the FNI function is arbitrary selected. The FNI function should not be confused with the admittance that is also denoted by the symbol (Y). The real and imaginary parts of the FNI function can be given in terms of the real and imaginary parts of the impedance (Szarka, 1994):

$$Y_r = (Z_r + Z_i) / \sqrt{2\omega\mu} \tag{3}$$

and

$$Y_i = (Z_i - Z_r) / \sqrt{2\omega\mu} \ . \tag{4}$$

For the horizontally stratified earth model, consisting of n homogeneous and isotropic layers of resistivities $\rho_1, \rho_2, ..., \rho_n$ and thicknesses $t_1, t_2, ..., t_n$, *Y* can be derived by following the conventional way described in textbooks (e.g. Kaufman and Keller, 1981):

$$Y = P_1 \tanh\{u\, t_1 / P_1 + \operatorname{arcth}(P_2 / P_1 . \tanh (u\, t_2 / P_2 + ... + \operatorname{arcth} [P_n / P_{n-1}])) ...\} \tag{5}$$

with

$$u = \sqrt{i\omega\mu} = (1+i)\sqrt{\mu\pi f} \tag{6}$$

and

$$P = \rho^{1/2} \ .$$

The above expression can be written as a recurrence formula

$$Y_m = P_m \tanh [ut_m / P_m + \operatorname{arcth} (Y_{m+1} / P_m)] \tag{7}$$

with

m = n-1, ...,2,1

and for substratum

$$Y_n = P_n \ . \tag{8}$$

Starting from the substratum, the new *Y* function can be found by adding a new layer at the top of the layer sequence.

The recurrent application of (7) gives the final *Y* function:

$$Y = Y_1 \ . \tag{9}$$

The recurrence expression (7) can also be written in the following equivalent forms (Basokur *et al.*, 1997a):

$$Y_m = P_m \frac{Y_{m+1} / P_m + \tanh (ut_m / P_m)}{1 + (Y_{m+1} / P_m) \tanh(ut_m / P_m)} \tag{10}$$

or

$$Y_m = \frac{Y_{m+1} + P_m \tanh (ut_m / P_m)}{1 + (Y_{m+1} / P_m) \tanh(ut_m / P_m)} \tag{11}$$

since

$$\tanh(a+b) = \frac{\tanh(a) + \tanh(b)}{1 + \tanh(a) \tanh(b)} \ . \tag{12}$$

APPARENT RESISTIVITY AND PHASE DEFINITIONS

The measured field quantities are usually converted to the apparent resistivity values in order to give physical significance to the data. The apparent resistivity defined by Cagniard(1953) has traditionally been used for the presentation of MT data. This definition can be given in terms of the real and imaginary parts of the FNI function as follows:

$$\rho_{aC} = \frac{1}{\mu\omega} |Z|^2 = Y_r^2 + Y_i^2 \tag{13}$$

where Y_r and Y_i are the real and the imaginary parts of the FNI function, respectively. Some definitions produce better results than the Cagniard's(1953) definition to reach true resistivities of the subsurface layers (Spies and Eggers, 1986). At present, the definition defined by Basokur(1994a) seems to be one of the most successful, giving apparent resistivity values close to the true resistivities of the layers and suppressing the oscillations of the MT curve which are not related to the features presented in the section.

The apparent resistivity definition, which can be applied to the descending branches of the real part of the FNI, is given as

$$\rho_{aF} = (Y_r - Y_i)^2 \tag{14}$$

and the apparent resistivity definition for the ascending branches of the real part is

$$\rho_{aF} = (Y_r^2 + Y_i^2)^2 / (Y_r + Y_i)^2 . \tag{15}$$

Since the sign of the imaginary part distinguishes between the descending and ascending branches, the

above definitions can be combined into a single equation (Basokur, 1994a):

$$\rho_{aF} = \left[(Y_r^2 - \text{sign} (Y_i) . Y_i^2) / (Y_r + Y_i) \right]^2 . \quad (16)$$

The above definition has been derived theoretically by making use of the properties of the FNI function. The reconciliation of this definition with the previously published definitions has been shown by Szarka(1994). He rewrites equations (14) and (15) in terms of the impedance as follows:

$$\rho_{aF} = \frac{2}{\omega\mu} Z_r^2 \quad \text{for } \phi_Z \geq \pi/4 \quad (17)$$

and

$$\rho_{aF} = \frac{1}{2\omega\mu} \frac{|Z|^2}{Z_i} \quad \text{for } \phi_Z \leq \pi/4 . \quad (18)$$

where ϕ_Z is the magnetotelluric phase and it is defined as

$$\phi_Z = \arctan(Z_i / Z_r) \quad (19)$$

where Z_r and Z_i represent the real and imaginary parts, respectively, of the impedance. After the Szarka's(1994) derivation, a little algebra leads to new equations for (14) and (15) in terms of the phase of impedance

$$\rho_{aF} = 2 \rho_{aC} \cos^2(\phi_Z) \quad \text{for } \phi_Z \geq \pi/4 \quad (20)$$

and

$$\rho_{aF} = \rho_{aC} / (2 \sin^2 (\phi_Z)) \text{ for } \phi_Z \leq \pi/4 . \quad (21)$$

The above pair of equations is equal to the definitions developed by Schmucker(1970). Now, it becomes clear that the equations (14), (20) and the definition of Spies and Eggers(1986) are exactly equivalent. The definition (15) is equivalent to the Schmucker's(1970) transformation given by (21). However, the comparison of the apparent resistivity definitions and theoretical explanation of their behaviour can easily be done by examining the FNI function.

The relation between the phases of the FNI and the impedance can be found from (2) as

$$\phi_Y = \phi_Z - \pi/4 \quad (22)$$

since

$$\text{phase} \left\{ 1/\sqrt{i\omega\mu} \right\} = -\pi/4 \quad (23)$$

As it is clear from (19 and (22), the shape of the phase curve is mainly controlled by the imaginary part of the FNI function. Thus, the behaviour of the MT phase can also be explained using the properties of the FNI function, namely by using the ratio of the imaginary and real parts of the FNI function.

BEHAVIOR OF THE FNI FUNCTION

As a first step, it is convenient to investigate the two-layer case to explain the behaviour of the real and imaginary parts of the *Y* function. From equation (7), the FNI function can be written as:

$$Y = P_1 \tanh\left((1+i)\sqrt{\mu\pi f} \, (t_1/P_1) + \text{arcth}(P_2 / P_1) \right). \quad (24)$$

If we denote

$$a = t_1 / P_1 . \sqrt{\mu\pi f} \quad (25)$$

and

$$b = \text{arcth}(P_2 / P_1) = 0.5 \ln(k) \quad (26)$$

with

$$k = (P_1 + P_2) / (P_1 - P_2), \quad (27)$$

we obtain

$$Y = P_1 \tanh((a + b) + ia) . \quad (28)$$

Knowing that

$$\tanh(x + iy) = \frac{\sinh(2x) + i \sin(2y)}{\cosh(2x) + \cos(2y)} , \quad (29)$$

we can separate the *Y* function into its real and imaginary parts that have the same denominator as follows:

$$Y = P_1 \left[\sinh(2a + 2b) / v + i \sin(2a) / v \right] \quad (30)$$

where

$$v = \cosh(2a + 2b) + \cos (2a) , \quad (31)$$

$$x = a + b ,$$

$$y = a .$$

By multiplying and dividing the right-hand side of (30) by cosh(2a + 2b), we can redefine the real and imaginary parts of the FNI function as follows:

$$Y_r = P_1 \; R(f) / D(f) \quad (32)$$

and

$$Y_i = P_1 \; I(f) / D(f) \quad (33)$$

where

$$R(f) = \tanh(2a + 2b), \quad (34)$$

$$I(f) = \sin(2a) / \cosh(2a + 2b) \quad (35)$$

and

$$D(f) = 1 + \cos(2a) / \cosh(2a + 2b). \quad (36)$$

From (25) and (26), we can prove that

$$\sinh(2a + 2b) = (c - 1/c) / 2, \quad (37)$$

$$\cosh(2a + 2b) = (c + 1/c) / 2 \quad (38)$$

and

$$\tanh(2a + 2b) = (c - 1/c) / (c + 1/c) \quad (39)$$

with

$$c = k \exp(2a). \quad (40)$$

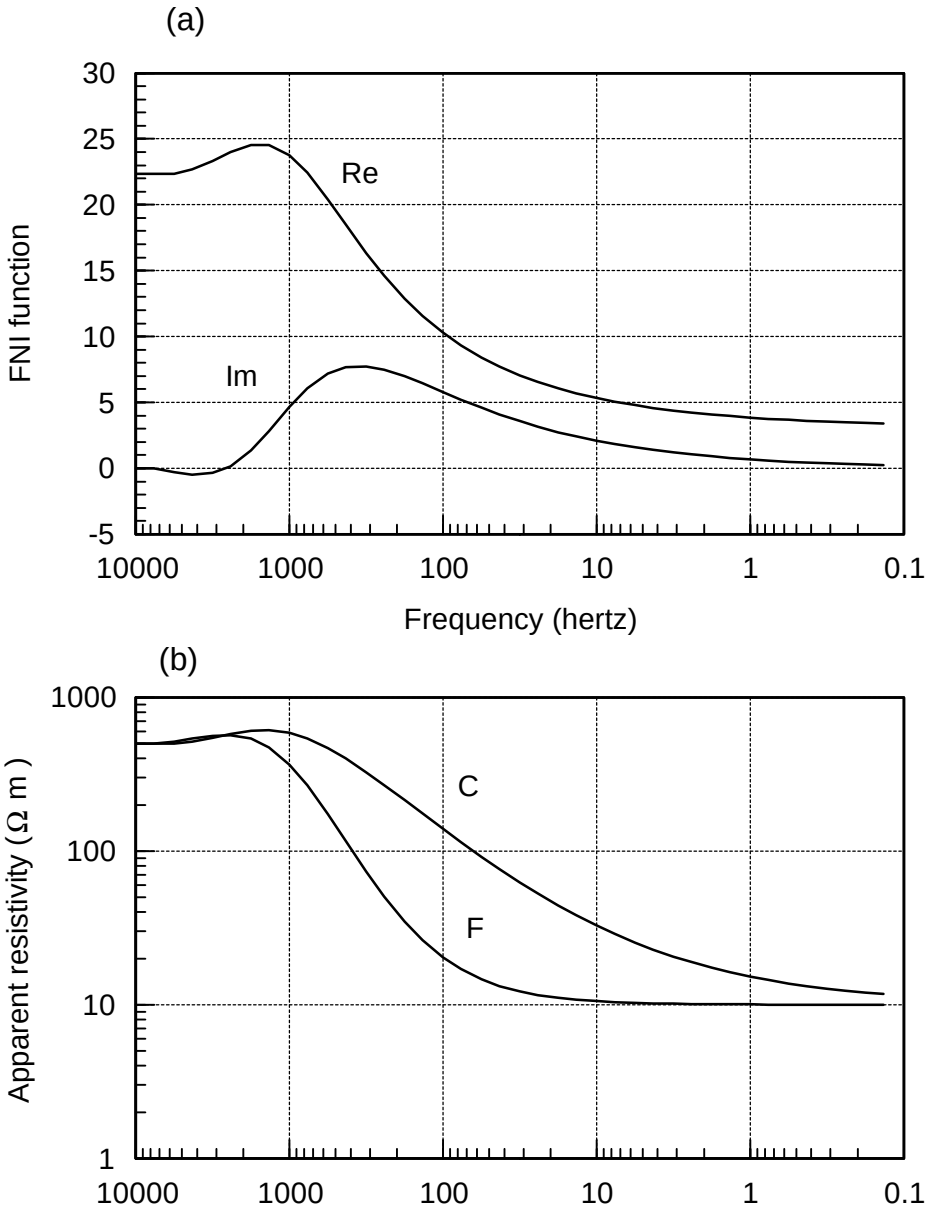

FIG. 1. (a) The real (Re) and the imaginary (Im) parts of the FNI function versus decreasing frequency for the model: ρ_1 = 500 ohm-m, ρ_2 = 10 ohm-m, t_1 = 350 m. (b) a comparison between Cagniard's apparent resistivity (C) and the apparent resistivity definition ρ_{aF} (F).

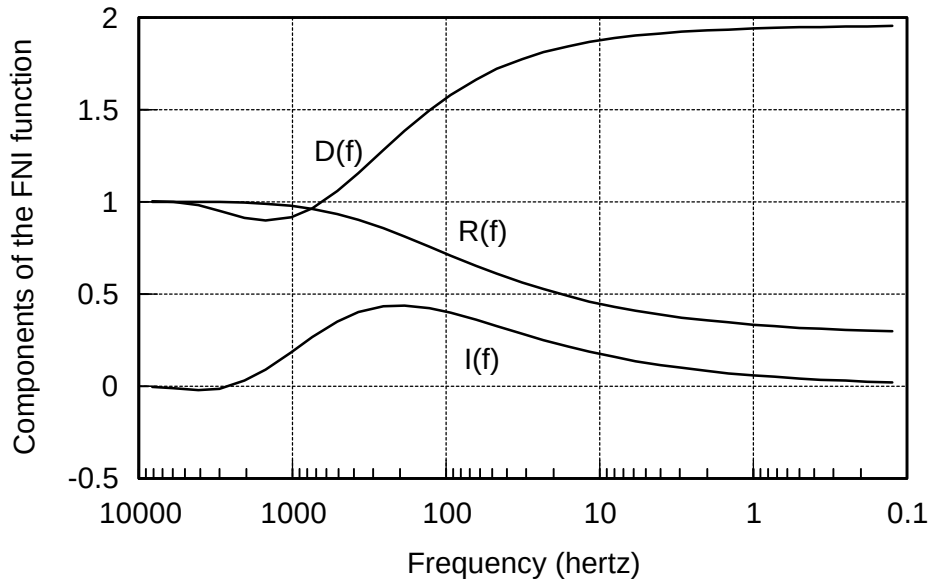

FIG. 2. Plots of the real R(f) and the imaginary I(f) parts of the FNI function versus decreasing frequency. D(f) is the denominator of the FNI function. The model is the same with Figure 1, but the sample values are normalised by the resistivity of the first layer.

These expressions lead to the analysis of the behaviour of the FNI function for descending and ascending types two-layer curves.

Descending Type Two-layer Curves

Figure 1a shows the real and imaginary parts of the FNI function computed for the case where the layer resistivities are 500 and 10 ohm-meters and the thickness of the top layer is 350 m. The behaviours of the real and imaginary parts can be analysed by the help of the previously defined R(f), I(f) and D(f) functions.

R(f) is equal to unity in the high frequency limit since tanh (∞)=1. The term cos(2a) in D(f) has positive numerical values except a few sample values at high frequencies where it becomes negative and consequently causes an oscillations in D(f) with smaller values than unity (Fig. 2). Y_r approaches the square root of the resistivity of the first layer since both R(f) and D(f) approach unity in the high frequency limit.

According to (27), k is positive and R(f) monotonously decreases with lowering frequency (Fig. 2). To find the numerical value of R(f) in the low frequency limit, we put f=0 into (40). By the help of (37) and (38) one finds:

$$R(f) = 2 P_1 P_2 / (P_1^2 + P_2^2) . \qquad (41)$$

In contrast to the behavior of R(f), the sample values of D(f) tend to increase with decreasing frequency since cosh(2a + 2b) has positive numerical values and it decreases with decreasing frequency (expression 36). If we put f=0 into (36) then we can find the following asymptotic value of D(f) by the help of (38) and (40) for the low frequency limit:

$$D(f) = 2 P_1^2 / (P_1^2 + P_2^2) . \qquad (42)$$

Substituting (41) and (42) into (32), we find that the real part of the FNI function equals to the square root of the resistivity of the second layer in the low frequency limit.

The real part of the FNI function consists of the division of a decreasing function (R(f)) by an increasing function (D(f)). As a result of this division, Y_r rapidly decreases in comparison with R(f). The oscillation on the D(f) is transferred to Y_r in reverse direction and Y_r has numerical values greater than the square root of the resistivity of the first layer at the abscissa range close to high frequency limit (Fig. 1a and Fig. 2).

The imaginary part of the FNI function becomes zero at high and low frequency limits (Fig. 1a). Because, the term cosh(2a + 2b) in I(f) has extremely high numerical values for high frequencies and consequently I(f) becomes zero. In the low frequency limit, the term sin(2a) in I(f) approaches zero (Fig. 2). At intermediate frequencies, the division sin(2a) / cosh(2a + 2b) is positive except the frequency range near high frequency limit where sin(2a) becomes negative. As mentioned before, D(f) also shows oscillatory behaviour in this frequency range. Since

I(f) has relatively small numerical values in this frequency range, the oscillation of the imaginary part of the FNI function is much smaller than that of the real part. After this oscillation near the high frequency limit, Y_i increases with decreasing frequency, passing through a maximum value it starts to decrease continuously and approaches zero at low frequency limit.

It is interesting to note that R(f) and I(f) are parallel to each other for relatively low frequency values (Fig. 2). This suggests that the difference between R(f) and I(f) is constant for small values of frequency. The following approximation is valid from (26) because $P_2 \langle P_1$ for this case:

$$b = \operatorname{arcth}(P_2 / P_1) \approx P_2 / P_1 . \quad (43)$$

We can also make the following approximations for small values of frequency:

$$R(f) = \tanh(2a + 2b) \approx 2a + 2b \quad (44)$$

and

$$D(f) = 1 + \cos(2a) / \cosh(2a + 2b) \approx 2 \quad (45)$$

since

$$\cos(2a) \approx 1 \quad (46)$$

$$\cosh(2a + 2b) \approx 1 \quad (47)$$

and

$$I(f) = \sin(2a) / \cosh(2a + 2b) \approx 2a . \quad (48)$$

If we subtract (48) from (44), we obtain

$$R(f) - I(f) \approx 2 b \approx 2 P_2 / P_1 . \quad (49)$$

This result explains why R(f) and I(f) remain parallel for the relatively small values of frequency (Fig. 2). Consequently, the same parallelism is also observed in the real and imaginary parts of the FNI function as can be seen on Fig. 1a. From (32) and (33) one finds that

$$Y_r - Y_i \approx P_1 (R (f) - I (f)) / D(f) . \quad (50)$$

If (45) and (49) are substituted into (50), then the differences of the real and imaginary parts of the FNI function becomes almost equal to the square root of the resistivity of the bottom layer:

$$P_2 \approx Y_r - Y_i . \quad (51)$$

This result explains the reason why the definition (14) is successful in reaching the true resistivity of the second layer at relatively high frequencies. Because of the structure of the definition (13), the Cagniard's(1953) definition could only reach the true resistivity of the substratum in low frequency limit where the imaginary and real parts of the FNI become equal to zero and the square root of the resistivity of the first layer. Since we have normally more than two layers, the contribution of deeper layers starts at intermediate frequencies and thus the Cagniard's(1953) definition never reaches the intrinsic resistivity of a layer. But, the definition (14) can attain the true resistivity of a layer before the contribution of the bottom layer starts. Figure 1b compares the behaviours of the apparent resistivity definitions.

Ascending Type Two-layer Curves

Figure 3a shows the real and imaginary parts of the FNI function computed for the case where the layer resistivities are 10 and 100 ohm-meters and the thickness of the top layer is 100 m. Since the resistivity of the second layer is greater than that of the first layer, k is negative. R(f) is equal to unity for high frequency values. The denominator D(f) is also equal to unity in the high frequency limit since cosh(2a + 2b) equals to infinity (Fig. 4). And the real part of the FNI function becomes equal to the square root of the resistivity of the first layer (Fig. 3a). (37) and (38) have always negative numerical values and consequently R(f) becomes decreasing function of lowering frequency.

The term cosh(2a + 2b) in the denominator D(f) has always negative values and its absolute values decrease with lowering frequency. The term cos(2a) generally has positive values except for the frequency values close to the high frequency limit. Then the division cos / cosh gives negative values with less than -1. Then D(f) becomes a decreasing function of lowering frequency. But, cos(2a) causes an oscillation on D(f) when it has negative values near high frequency limit where D(f) becomes greater than unity for a few sample values (Fig. 4).

The real part of the FNI function is obtained by dividing R(f) to D(f) which both of them are decreasing functions of lowering frequency. However, D(f) decreases rapidly than R(f) and the final division gives an increasing function of decreasing frequency. The oscillation of D(f) due to the term cos(2a) also causes an oscillation on the real part of the FNI function in the reverse direction where the sample values of the FNI function become less than P_1 (Fig. 3a). Cagniard apparent resistivity also shows oscillating behaviour at the same sample points as slightly smaller apparent resistivity values than the true resistivity of the first

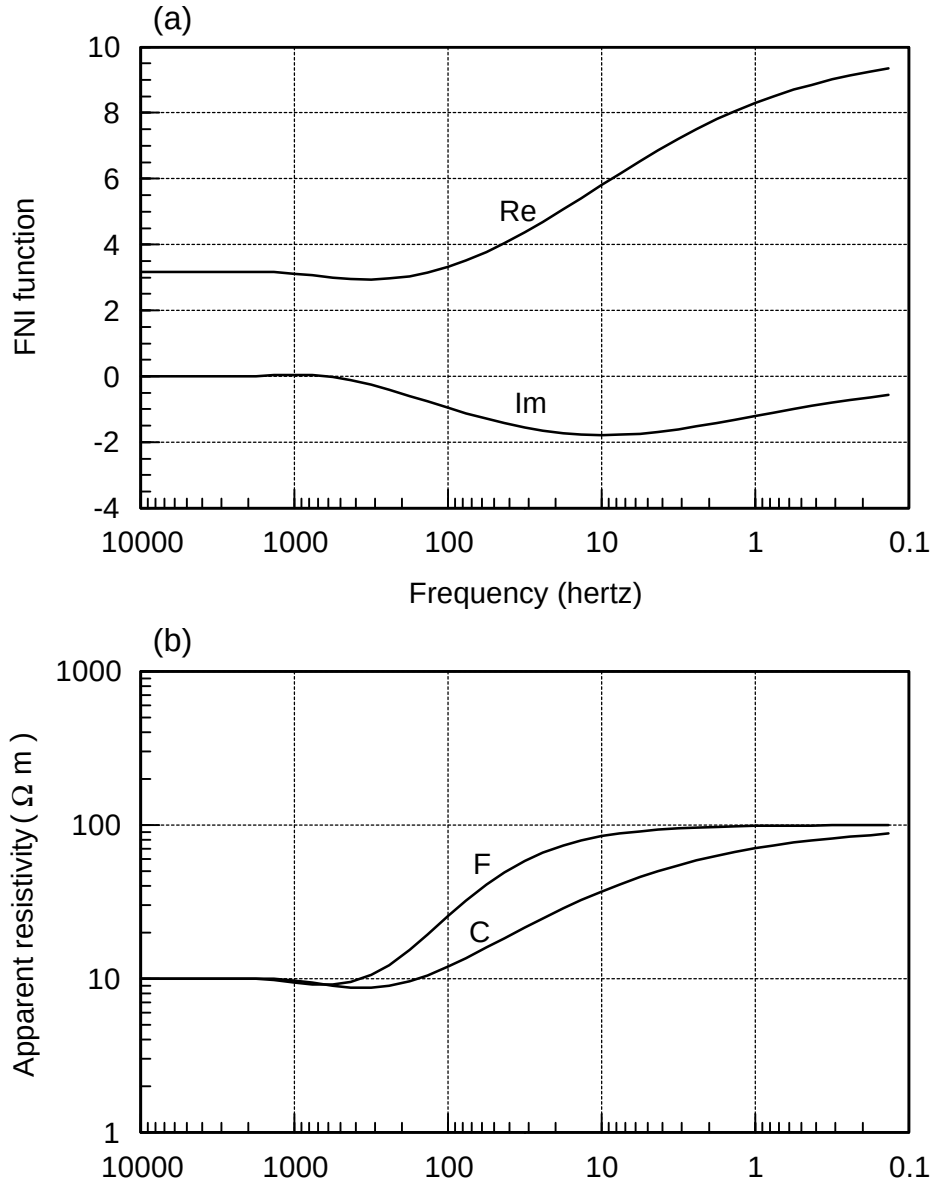

FIG. 3. (a) The real (Re) and the imaginary (Im) parts of the FNI function versus decreasing frequency for the model: ρ_1 = 10 ohm-m, ρ_2 = 100 ohm-m, t_1 = 100 m. (b) a comparison between Cagniard's apparent resistivity (C) and the apparent resistivity definition ρ_{aF} (F).

layer because of the same reason.

As in the case of descending type curves, the real part of the FNI function approaches the square root of the resistivity of the substratum in the low frequency limit. Expressions (41) and (42) are also valid for this case.

The numerator of the imaginary part of the FNI function I(f) becomes zero in high and low frequency limits (Fig. 4). Because, cosh(2a + 2b) has extremely high numerical values for high frequencies and consequently I(f) becomes zero. In low frequency limit, I(f) is zero since sin(2a) becomes zero for very small frequency values. At intermediate frequencies, the division sin(2a) / cosh(2a + 2b) becomes negative because sin(2a) is positive except the frequency range close to high frequency limit where D(f) also shows oscillatory behaviour.

Since the magnitude of D(f) is greater than I(f), the final division (35) results that the absolute values of the imaginary part of the FNI function is always less than that of the real part except perfectly insulating and conducting substratum cases. And also the magnitude of the oscillation on the imaginary part is smaller than that of real part. Due to the same reason, the magnitude of oscillation of the phase becomes relatively smaller than that of the Cagniard apparent resistivity.

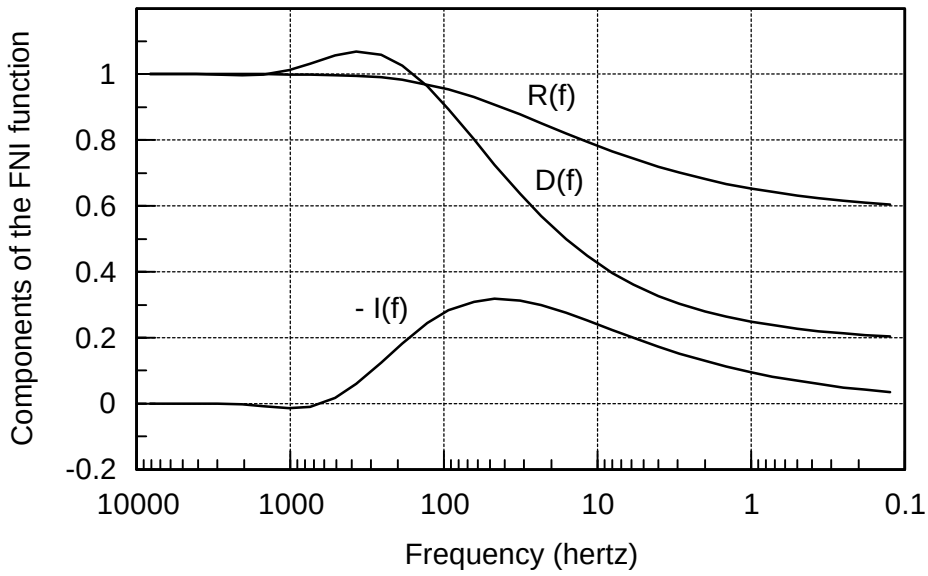

FIG. 4. Plots of the real R(f) and the imaginary I(f) parts of the FNI function versus decreasing frequency. D(f) is the denominator of the FNI function. The imaginary part is multiplied by -1. The model is the same with Figure 3, but the sample values are normalised by the resistivity of the first layer.

Finally, we see that if the resistivity of the second layer is greater than that of the first layer, the imaginary part of the FNI function is zero at high and low frequency limits. At intermediate frequencies, it is negative and it decreases with lowering frequency, passing though a minimum value and then reaches zero in low frequency limit except the relatively small oscillation at high frequencies.

Similar to descending type two-layer curves, we can try to estimate the resistivity of substratum by using the sample values of the real and the imaginary part of the FNI function. However, the approximations from (43) to (51) are not valid for this case since $P_1 \langle P_2$. To determine the resistivity of the second layer, the concept of the 'reciprocal geoelectric section' can be used (Basokur, 1994b). This section is obtained when

$$\rho_1^{\backslash} = 1/\rho_1 \tag{52}$$

$$\rho_2^{\backslash} = 1/\rho_2 \tag{53}$$

$$t_1^{\backslash} = t_1/\rho_1 \tag{54}$$

replace the original parameters. Taking into account the following property

$$\tanh[z + \operatorname{arcth}(w)] = 1/\tanh[z + \operatorname{arcth}(1/w)] \tag{55}$$

and in view of (28), one finds

$$Y_r^{\backslash} + iY_i^{\backslash} = 1/(Y_r + iY_i)\,. \tag{56}$$

Multiplying and dividing the right-hand side of the above equation by the conjugate of the denominator, we can obtain the real and imaginary parts of the FNI function for the reciprocal geoelectric section as follows:

$$Y_r^{\backslash} = Y_r / (Y_r^2 + Y_i^2) \tag{57}$$

and

$$Y_i^{\backslash} = -Y_i / (Y_r^2 + Y_i^2)\,. \tag{58}$$

Now, we can apply the approximations from (43) to (51) to the reciprocal geoelectric section. According to (51), we write

$$P_2^{\backslash} \approx Y_r^{\backslash} - Y_i^{\backslash}\,. \tag{59}$$

We can turn back to original geoelectric section by considering the reciprocal section of the equation (59). Substituting (53), (57) and (58) into (59), one finds

$$P_2 \approx (Y_r^2 + Y_i^2)/(Y_r + Y_i)\,. \tag{60}$$

This equation serves to estimation of the resistivity of the second layer by using the sample values of the FNI function at intermediate frequencies. However, in the high frequency limit, Y_i is zero and (60) becomes equal to the square root of the resistivity of the first layer. Since the apparent resistivity definition (15) and the equation (60) equal to each other, one can expect that the definition (15) would give apparent resistivity

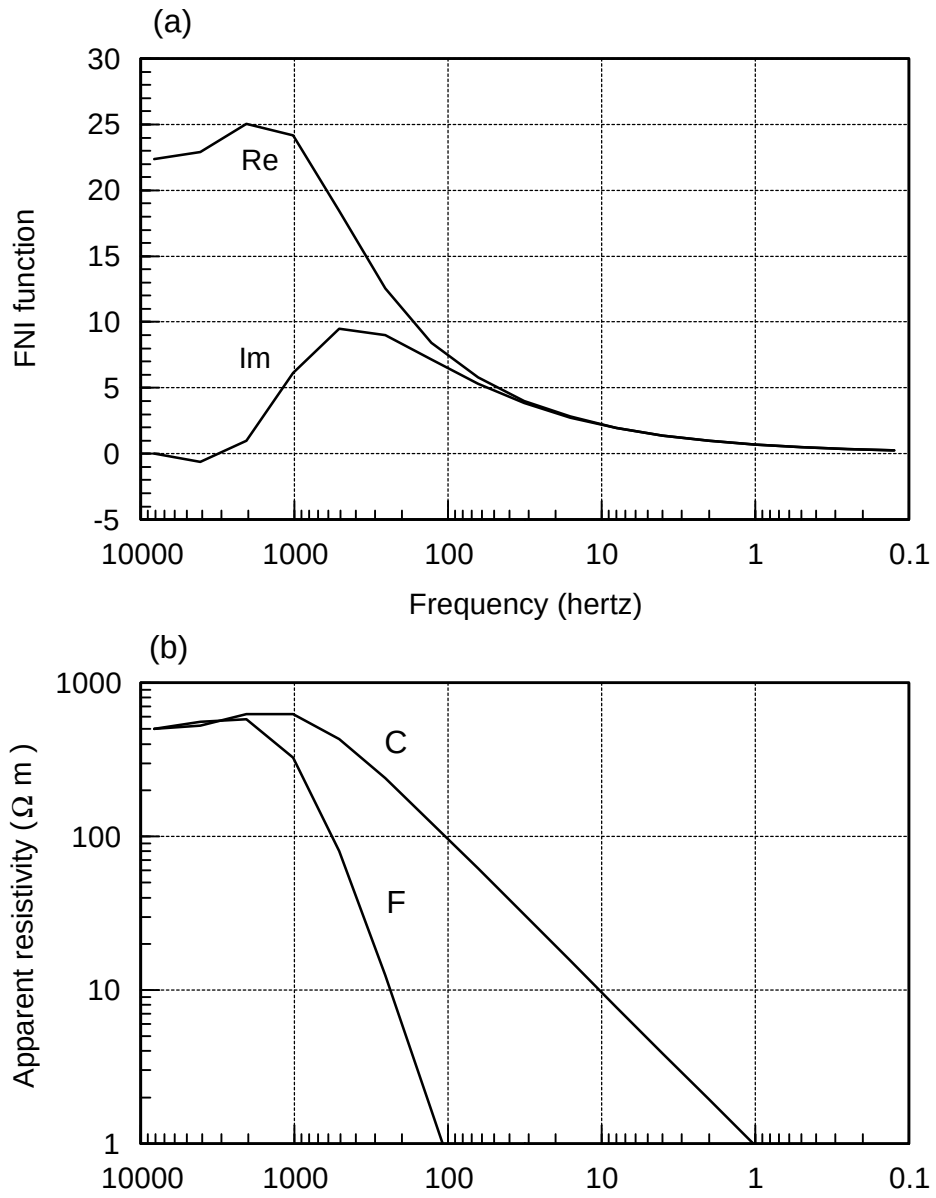

FIG. 5. a) The FNI function versus decreasing frequency for the perfectly conducting substratum case where the model: ρ_1 = 500 ohm-m, ρ_2 = 0 ohm-m, t_1 = 350 m. (b) a comparison between Cagniard's apparent resistivity (C) and the apparent resistivity definition ρ_{aF} (F).

values very close to the true resistivities of the subsurface layers in case of ascending branches.

Perfectly Conducting and Insulating Substratum

In the case of perfectly conducting substratum ($\rho_2 = 0, P_2 = 0$), one can prove that the coefficient k is equal to unity by substituting P_2 = 0 into (27). In view of (37), (38) and (40), the numerator and the denominator of the real part become

$$R(f) = \sinh(2a) / \cosh(2a) \quad (61)$$

and

$$D(f) = 1 + \cos(2a) / \cosh(2a). \quad (62)$$

From (35) the numerator of the imaginary part can be written as follow:

$$I(f) = \sin(2a) / \cosh(2a). \quad (63)$$

It can be proved that the real and the imaginary parts of the FNI function are equal to each other for sufficiently low frequency values:

$$Y_r = Y_i \quad (64)$$

since

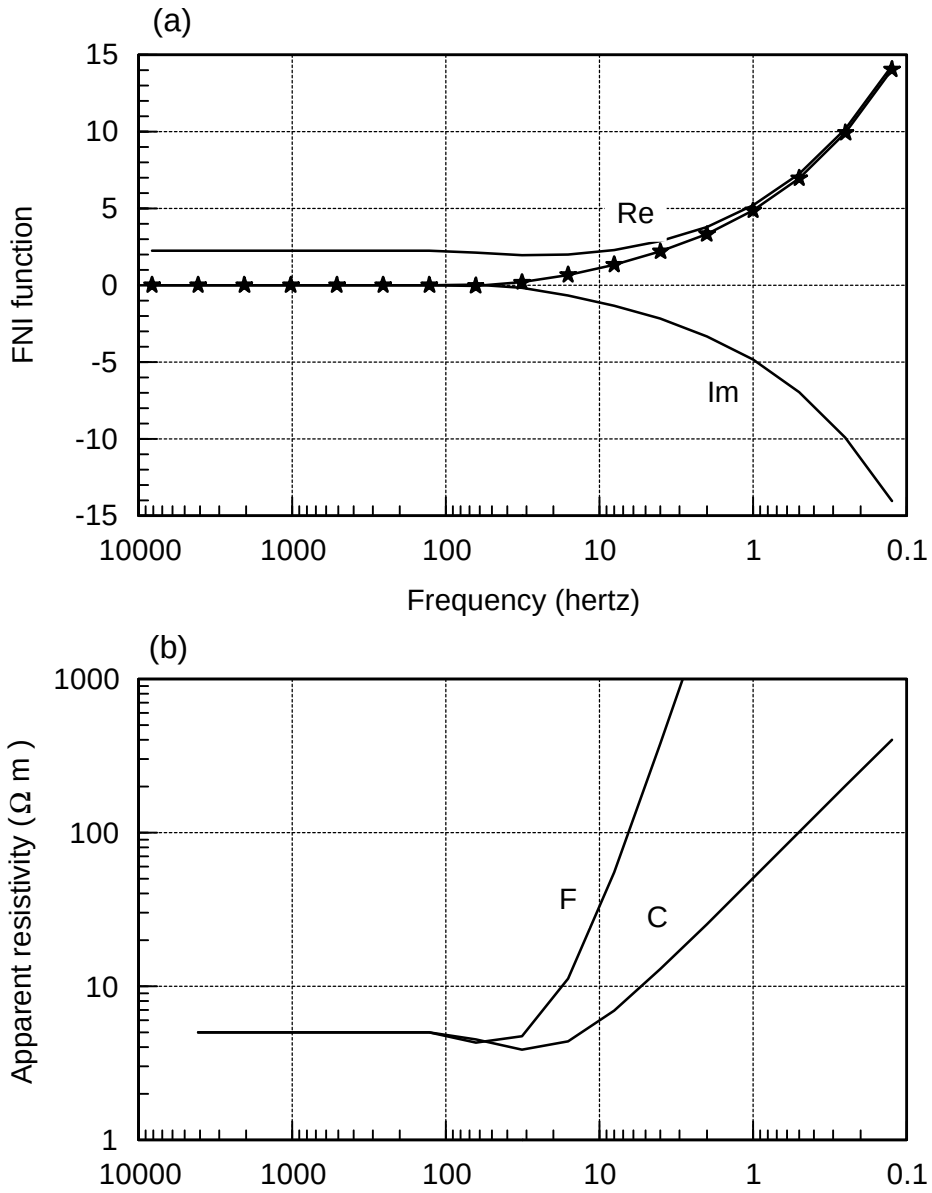

FIG. 6. (a) The FNI function versus decreasing frequency for the perfectly insulating substratum case where the model: ρ_1 = 500 ohm-m, $\rho_2 = \infty$ ohm-m, t_1 = 350 m. The stars show the absolute values of the imaginary part approaching to the real part for high frequency values. (b) a comparison between Cagniard's apparent resistivity (C) and the apparent resistivity definition ρ_{aF} (F).

$$\sin(2a) \approx 2a$$

and

$$\sinh(2a) \approx 2a ,$$

for small values of *2a* (Fig. 5a). The difference between the real and the imaginary parts becomes zero and equals to the resistivity of the second layer as defined by (51) or (14).

In the case of insulating basement ($P_2 = \infty$), (27) can be written in the following form by dividing both numerator and denominator by P_2 :

$$k = (P_1 / P_2 + 1) / (P_1 / P_2 - 1) \qquad (65)$$

Since $P_2 = \infty$ then k becomes equal to -1. Putting k= -1 into (40) and (41), we obtain

$$-\sinh(2a) = - (\exp(2a) - 1 / \exp(2a)) \qquad (66)$$

and

$$-\cosh(2a) = - (\exp(2a) + 1 / \exp(2a)) \qquad (67)$$

and the numerator and the denominator of the real part become

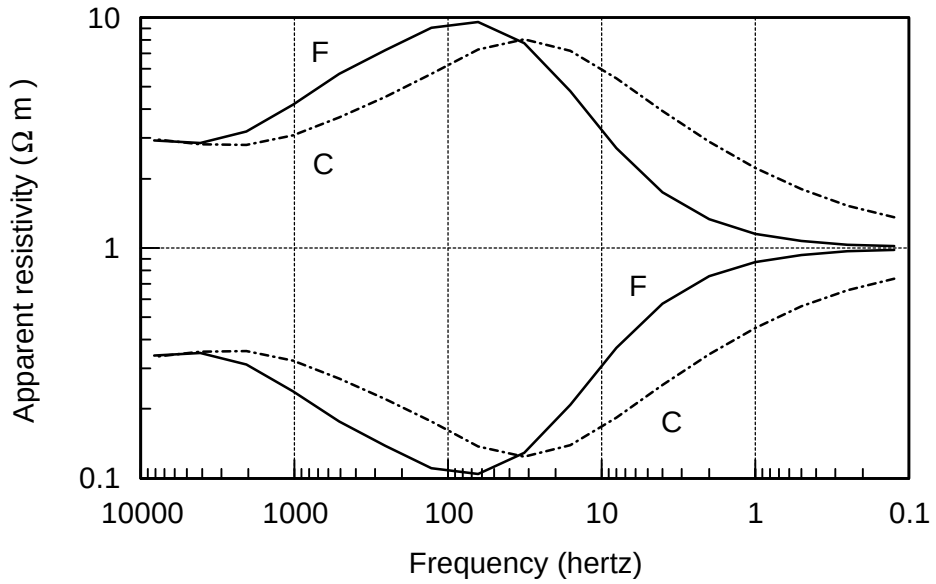

FIG. 7. (a) Symmetry of apparent resistivity curves with respect to the horizontal axis $\rho_a = 1$. C and F indicate Cagniard's apparent resistivity and the apparent resistivity definition ρ_{aF}, respectively. The upper curves are computed for the model: $\rho_1 = 3$ ohm-m, $\rho_2 = 10$ ohm-m, $\rho_3 = 1$ ohm-m, $t_1 = 20$ m, $t_2 = 250$ m. The lower curves of the corresponding reciprocal geoelectric section are computed for the model: $\rho_1 = 1/3$ ohm-m, $\rho_2 = 0.1$ ohm-m, $\rho_3 = 1$ ohm-m, $t_1 = 20/3$ m, $t_2 = 25$ m.

$$R(f) = \sinh(2a)/\cosh(2a), \quad (68)$$

$$D(f) = 1 - \cos(2a)/\cosh(2a). \quad (69)$$

The numerator of the imaginary part can be written in similar way as

$$I(f) = -\sin(2a)/\cosh(2a). \quad (70)$$

For small values of frequency, the imaginary part is negative and its absolute values are approximately equal to the real part (Fig 6a):

$$R(f) \approx -I(f) \quad (71)$$

or

$$Y_r \approx -Y_i \quad (72)$$

since

$-\sin(2a) \approx -2a$,

$\sinh(2a) \approx 2a$.

(72) can also be proved by using the concept of reciprocal geoelectric section. The perfectly insulating substratum case is the reciprocal section of perfectly insulating case and vice-versa. By the help of (57), (58) and (64) and by using the properties of the reciprocal section, (72) can also be obtained.

The situation can easily be seen in Fig. 6a. The absolute values of the imaginary part are plotted as continuous curve to show how the imaginary part reaches to the real part. In that way, we prove the robustness of (15). Due to (72), the denominator of (15) becomes zero for this case and consequently the apparent resistivity definition (15) tends to approach infinity.

These results show that the magnitude of the imaginary part of the FNI function varies between zero and the magnitude of the real part depending on the resistivity ratio of layers. It is zero if there is no contrast. This corresponds to homogenous earth case. The earth also behaves like homogeneous earth in high frequency limit where the second layer has no contribution on the FNI function. After reaching a maximum or a minimum value the imaginary part becomes zero at low frequency limit.

RECIPROCAL PROPERTY OF APPARENT RESISTIVITY

As defined before, the reciprocal geoelectric section is obtained when the resistivity values of the subsurface layers are replaced by their reciprocals.

The thicknesses of the corresponding reciprocal geoelectric section are equal to the thicknesses divided by the resistivities of those layers. The equations (57) and (58) give the relation between the real and imaginary parts of the FNI function and the FNI function of the corresponding reciprocal section. The sample values of the corresponding reciprocal apparent resistivity definitions can easily be found from (57) and (58). The results are:

$$\rho_{aC} = 1 / \rho'_{aC} \tag{73}$$

and

$$\rho_{aF} = 1 / \rho'_{aF} \tag{74}$$

These equations show that the bilogarithmic plot of the apparent resistivity curves will be symmetric with the apparent resistivity curves of the corresponding reciprocal section. The axis of symmetry is the horizontal axis that intersects the vertical axis at unity. Figure 7 shows the symmetries of the apparent resistivity curves and their reciprocals with respect to the horizontal axis of apparent resistivity equals to unity.

CONCLUSIONS

The examination of the FNI curves gives useful information about the resistivity distribution of the subsurface layers. The sample values of the real part of the FNI function vary within the range of the square root of the true resistivity values. The ascending and descending branches of the real part indicate the transition from one layer to the next. A semi-circular shaped arc on the imaginary part represents a boundary between two consecutive layers.

In most cases, the magnitude of the real part is higher than that of the imaginary part. Consequently, the contribution from the real part is dominant when calculating the apparent resistivity using Cagniard's(1953) definition. Then, a significant part of the information contained in the imaginary part is lost. For this reason, the effects of the relatively thin layers on the Cagniard's(1953) apparent resistivity curves become invisible. Moreover, the oscillations of the real part are transferred to the apparent resistivity curve. But, these oscillations are suppressed in the ρ_{aF} definition, and the effect of the true resistivity values of the layers is magnified. Because, the imaginary part compensates the oscillations caused by the real part.

The apparent resistivity definitions are useful for the qualitative interpretation of the MT data. A practical application has been described by Basokur *et al*. (1997b) for a massive sulphide exploration problem. The examination of the real and imaginary parts of the FNI function also give useful information and seems to be more feasible than the apparent resistivity data for the quantitative interpretation. Using the FNI formulation instead of the apparent resistivity and the phase values may carry the inversion of the MT data more efficiently in comparison with the conventional procedures (Ulugergerli and Basokur, 1994).

ACKNOWLEDGMENTS

This work supported by the Scientific and Technical Research Council of Turkey (TUBITAK) under grant no. YBAG-102.

REFERENCES

Basokur, A. T., 1994a, Definitions of apparent resistivity for the presentation of magnetotelluric sounding data: Geophysical Prospecting, **42**, 141-149.

Basokur, A. T., 1994b, Reply to Comment on 'Definitions of apparent resistivity for the presentation of magnetotelluric sounding data' by L. Szarka: Geophysical Prospecting, **42**, 989-992.

Basokur, A. T., Kaya, C. and Ulugergerli, E. U., 1997a, Direct interpretation of magnetotelluric sounding data based on the frequency-normalized impedance, Geophysical Prospecting, 43, 17-34

Basokur, A. T., Rasmussen, T. M., Kaya, C., Altun, Y., Aktas, K., 1997b, Comparison of Induced Polarization and Controlled Source Audio-Magnetotellurics methods for the massive chalcopyrite exploration in volcanic area, Geophysics 62, 1087-1096

Cagniard, L., 1953, Basic theory of the magnetotelluric method of geophysical prospecting: Geophysics, **18**, 605-635.

Kaufman, A. A., Keller, G.V., 1981, The magnetotelluric sounding method: Elsevier.

Schmucker, U., 1970, Anomalies of geomagnetic variations in the southwestern United States: Scripps Institution of Oceanography Bulletin, **13**, Univ. of California Press, 165 pp.

Spies, B.R., Eggers, D.E., 1986, The use and misuse of apparent resistivity in electromagnetic methods: Geophysics, **51**, 1462-1471.

Szarka, L., 1994, Comment on 'Definitions of apparent resistivity for the presentation of magnetotelluric sounding data' by A. T. Basokur': Geophysical Prospecting, **42**, 987-988.

Ulugergerli, E. U. and Basokur, A.T., 1994, Effect of the type of data on the solution of layer parameters in magnetotelluric inversion (in Turkish), Jeofizik, **8**, 123-146.